



Clay nanofiller enhances and stabilises a new injectable human bone extracellular matrix scaffold for skeletal regeneration

Gianluca Cidonio^{a,b,c}, Vikash H. Dodhia^a, Lucia Iafrate^c, Janos M. Kanczler^a, Julietta V. Rau^d, Valeria Giliberti^c, Alessandro Nucara^e, Richard O.C. Oreffo^a, Jonathan I. Dawson^{a,*}, Yang-Hee Kim^{a,*}

^a Bone and Joint Research Group, Centre for Human Development, Stem Cells and Regeneration, Institute of Developmental Sciences, Faculty of Medicine, University of Southampton, Southampton SO16 6YD, United Kingdom

^b Department of Mechanical and Aerospace Engineering, Faculty of Civil and Industrial Engineering, Via Eudossiana 18, Rome 00184, Italy

^c Center for Life Nano, & Neuro-Science (CLN2S), Fondazione Istituto Italiano di Tecnologia, Viale Regina Elena 291, Rome 00161, Italy

^d Istituto di Struttura della Materia, Consiglio Nazionale delle Ricerche (ISM-CNR), Via del Fosso del Cavaliere 100, Rome 00133, Italy

^e Department of Physics, University of Rome "La Sapienza", Piazzale Aldo Moro 5, Rome 00185, Italy

ARTICLE INFO

Keywords:

Bone
Decellularization
Injectable
Hydrogel
Nanocomposite

ABSTRACT

Critical bone defects and fractures are typically treated using autologous bone grafts, which are limited by volume of bone that can be harvested, or allogeneic or synthetic bone grafts that lack osteoinductive properties. Human bone extracellular matrix (hbECM) is widely available and offers the potential to be used as a native material to synthesize functional injectable hydrogel systems. However, hbECM lacks the mechanical stability required for injectability and bone growth. We have explored the use of Laponite® (LAP) nanoclay and sodium polyacrylate to augment the mechanical and biological properties of hbECM gel. We demonstrated that the inclusion of LAP into ECM improved the physicochemical properties of hbECM and consequently promoted cell responses confirming that the nanoclay platelet-to-platelet interaction is key to sustain hbECM functionality. This novel hbECM detailed offers significant clinical promise for bone repair.

1. Introduction

Musculoskeletal disorders are currently the most common cause of disability worldwide [1]. Fractures alone cost the European economy €17 billion and the US economy \$20 billion annually [2,3]. Autologous bone grafts are clinically applied for the treatment of large bone defects. However, current issues on graft remodelling and the lack of sufficient autologous material preclude universal application. While allogeneic bone holds potential risks of cell-mediated immune responses and contamination, clinical alternatives such as synthetic scaffolds lack the desired osteoinductivity to facilitate bone regeneration [4]. Tissue engineering and regenerative medicine (TERM) have sought to address the need for bone augmentation using synthetic or biological, biocompatible and biodegradable materials capable of guiding tissue regeneration. Gel-based materials can be engineered to provide injectable constructs with the potential for minimally-invasive delivery of cellular and therapeutic components [5,6]. However, the inert nature of popular

materials (e.g., alginate), the inability to support functional tissue regeneration and the lack of control over the gelation properties following injection have, to date, limited the clinical translation of a number of injectable materials. Nevertheless, injectable systems can be engineered to mimic extracellular matrix (ECM) features and properties, facilitating integration and preventing a foreign body response. With the optimal formulation of extracellular proteins and polymers (e.g., collagen, laminin, fibronectin), ECM offers functional sites for cell attachment and proliferation, while encapsulating growth factors capable of modulating cell fate [7,8].

Biomaterials derived and prepared from native tissues are attractive given their capacity to mimic elements of the natural biochemical/physical environment [9]. Indeed, demineralised bone matrix (DBM) has been shown for more than 60 years to hold osteoinductive potential when devitalised and decalcified [10]. However, unlike DBM, new immune-privileged materials have come to the fore providing new acellular platforms for tissue regeneration. ECM-based materials have

* Corresponding authors.

E-mail addresses: jid@soton.ac.uk (J.I. Dawson), yanghee.kim@soton.ac.uk (Y.-H. Kim).

<https://doi.org/10.1016/j.mtcomm.2024.109082>

Received 23 December 2023; Received in revised form 19 April 2024; Accepted 29 April 2024

Available online 30 April 2024

2352-4928/© 2024 The Authors. Published by Elsevier Ltd. This is an open access article under the CC BY license (<http://creativecommons.org/licenses/by/4.0/>).

been previously proposed for tissue regeneration, with modest success using xenogeneic-sourced materials such as the porcine small intestinal submucosal ECM for soft-tissue repair [11,12]. ECM from bone tissue has proved challenging to isolate and the limited availability of human tissue has led to a focus on animal-based ECM gels, although there are clear species differences therein. Moreover, the resultant lack of studies on human bone ECM has made evident the need for studies on the regenerative potential for skeletal tissue following decellularization and demineralization. Nevertheless, the poor rheological and mechanical stability have negatively impacted the pre-clinical use of ECM-based injectable materials. Nanofillers have been used to rapidly modify the injectability of a number of polymers. Particularly, Laponite® (LAP) nanoclay are an excellent candidate for conferring shear thinning properties to blended polymers [13,14]. Injectability of nanocomposites can be modified by altering surface charge interaction with sodium polyacrylate (ASAP) as previously demonstrated [15,16]. However, the physicochemical modification of ECM-based materials with LAP and ASAP has never been reported and yet remain to be studied.

We report an innovative injectable nanocomposite ECM-based gel capable of driving osteogenic regeneration supporting rapid delivery *in situ*, gelation under physiological conditions and mineralization depending on the nanoclay and surfactant concentration.

2. Materials and methods

2.1. Nanoclay-based material preparation

Nanoclay gels were prepared dispersing 1.4 % w/v UV sterile LAPONITE® XLG (LAP, BYK Ltd, UK) in deionised water followed by a constant stirring for 3 h. A series of concentrations (0, 0.06 and 0.12 %) of sodium polyacrylate (ASAP, MW:15,000, 35 wt %, Sigma-Aldrich, UK) were added to LAP suspension following stir at room temperature for 3 h.

2.2. Human bone extracellular matrix

Human bone extracellular matrix (hbECM) hydrogel was synthesised following as previously described [17,18]. Briefly, trabecular bone was isolated from adult femoral heads collected from haematologically normal patients undergoing routine elective hip replacement surgery. Only tissue samples that would have been discarded were used following informed consent from the patients in accordance with approval from Southampton & Southwest Hampshire Local Research Ethics Committee (Ref: 194/99/w). Bone tissue was ground and separated collecting fragments which were demineralised under agitation with 0.5 N HCl for 24 h. Any remaining lipid was removed with a 1:1 mixture of HCl and methanol and washed repeatedly. The bone fragments were then frozen and lyophilised overnight. Decellularization was carried out under agitation in a 0.05 % Trypsin/0.02 % EDTA mixture at 37°C for 24 h. The solution was then dried through vacuum filter and washed repeatedly with PBS before further lyophilization. The material was further digested in pepsin solution (1 mg/ml in 0.01 N HCl) for 7 days. The digested solution was then centrifuged at 2000 rpm for 15 min and supernatant collected, neutralised using the combination of NaOH and PBS and incubated overnight to collect the final ECM hydrogel (hbECM) at a concentration of 20 mg ml⁻¹.

2.3. Nanocomposite preparation

LAP suspensions (2.8 %) treated with various concentrations of ASAP were blended with hbECM supernatant (20 mg ml⁻¹) at 1:1 ratio (in brief, ECM-based Laponite® suspension (ELAP)), neutralising the solution following vortex agitation for 10 s. To allow complete setting, nanocomposite blends (Table 1) with 0 % (ELAP0), 0.06 % (ELAP6) and 0.12 % (ELAP12), respectively, were incubated at 37°C overnight. hbECM (10 mg ml⁻¹) and LAP (1.4 %) gels on their own were used as

Table 1
Nanocomposite polymeric concentrations.

Composites	hbECM	Nanoclay	ASAP
ELAP0	10 mg ml ⁻¹	1.4 %	0 %
ELAP6	10 mg ml ⁻¹	1.4 %	0.06 %
ELAP12	10 mg ml ⁻¹	1.4 %	0.12 %

controls.

2.4. Scanning electron microscope (SEM)

Morphology images were acquired using a Zeiss 300 FE scanning electron microscope (SEM) (Carl Zeiss, Oberkochen, Germany) at 4 kV EHT. ImageJ software (version 1.53 t) was applied to analyse micrographs.

2.5. Fourier transform infrared spectroscopy (FTIR)

Measurements have been performed in vacuum with a Fourier transform infrared (FTIR) spectrometer (Vertex 66 by Bruker) equipped with a single-reflection diamond crystal attenuated total reflectance (ATR) accessory (by Pike Technologies), a DTGS detector and a KBr beam-splitter. A pressure clamp with a flat tip was used to accommodate and press the samples on the diamond crystal. The ATR-FTIR absorption spectra have been obtained from the transmission spectrum T as $-\log(T)$ and no ATR correction has been done on the spectra.

2.6. Rheological measurements

Amplitude sweeps with an increasing shear strain (0.01–100 %) at a constant angular frequency of 10 s⁻¹ at 37°C was carried out on gels loaded on a cone plate rheometer (MCR92, Anton Parr). A constant strain measurement was performed following setting protocol performed with 3 ml of fetal bovine serum (FBS) to surround the gel following 2 min of measurement.

2.7. Gel degradation

To evaluate the degradation of nanocomposite gels, 50 µL of pre-set nanocomposite and control (hbECM and Nanoclay) gels were incubated in PBS for 24 hours, and then further incubated in collagenase-PBS (100 µg ml⁻¹) for 24 hours. The supernatants were collected at each time point (1, 2, 6, 24, 25, 26, 30, and 48 h) and kept in –20 °C until use. The proteins in supernatants were quantified with Fluoroprofile Protein Quantification Kit (Sigma FP0010). The pH in PBS and collagenase-PBS was measured by Mettler Toledo pH meter (Bioclass, Italy) and the weight loss of composites during the 48-hour incubation was calculated based on the initial weight of the dried composite gels.

2.8. Turbidimetric assay

Turbidity of 100 µL gels was measured at a wavelength of 450 nm using a microplate reader (Glomax, Promega) at 37°C every 2 minutes for 1 hour.

2.9. Cell differentiation

Mouse myoblast (C2C12) cells were seeded (2×10^5 cells/well) onto 10 µL dried gels (or empty control wells) and allowed to attach. Gels were loaded with increasing concentrations of bone morphogenetic protein-2 (BMP-2: 0, 100, 200, 400 ng ml⁻¹). Following a 72 h culture, cells were fixed and stained with Alkaline Phosphate (ALP) solution following standard protocols [19]. Samples were imaged at 10x magnification and photographed. Image analysis was performed using Cell Profiler quantifying the ALP intensity on n=5 image set for each

treatment group.

2.10. Statistics

All statistical analysis was performed on GraphPad Prism 9 (GraphPad Software, LLC, version 9.0.1). Results are reported as mean \pm SD. P value < 0.05 was considered as statistically significant between different experimental sets with one-way and two-way ANOVA.

3. Results and discussion

Following a published human bone ECM synthesis protocol [20] bone fragments were isolated and digested to decellularize and demineralize the matrix (Fig. 1a). Nanoclay suspensions were subsequently blended with hbECM following selective inclusion of ASAP ranging from 0 % (ELAP0), 6 % (ELAP6) up to 12 % (ELAP12) to obtain a homogeneous suspension (Fig. 1b).

3.1. Clay addition facilitated the packing of a loose ECM network

To investigate the morphological appearance and microscopical arrangement of clay combined with ASAP and hbECM, SEM images were acquired (Supplementary Fig. 1). Clay materials (Supplementary Fig. 1a) appeared as lamellae, while hbECM (Supplementary Fig. 1b) resembled the trabecular network of native bone at scale, with open pores and interconnectivity. However, when clay and hbECM were combined with increasing concentrations of ASAP (Supplementary Figure 1c-e) the structured appeared more compact, with no visible differences at the microscopic level.

The analysis of the microstructural arrangement of composites carried out with a Fourier transform infrared (FTIR) spectrometer, revealed the spectra of main characteristic absorption peaks of Laponite and bECM materials, with assignment of the main bands reported in

Supplementary Fig. 2a.

Supplementary Fig. 2b demonstrate the ATR-FTIR absorption spectrum for the three composites with increasing ASAP content. The ELAP curves have been normalized at the maximum of the amide-I band falling around 1660 cm^{-1} . All three composite materials clearly show the typical absorption bands of both Laponite and bECM (insert on the right for a zoom in the $1200\text{--}1800\text{ cm}^{-1}$) confirming the successful inclusion and presence of the two components in a tight network with ASAP. Moreover, it is evident from the analysis reported in Supplementary Fig. 2c, that the relative intensity of the clay absorption peaks increases with the increase of the ASAP content. This is confirmed by the reported ratio between the intensity at 980 cm^{-1} and that at 1660 cm^{-1} , demonstrating the rapid and effective shielding of the positive charges of the clay nanodiscs already saturated at 0.6 % ASAP.

3.2. Clay nanoparticles improved rheological properties of hbECM

To test the utility of LAP to enhance the rheological properties of hbECM, the nanoclay was blended at a fixed ratio to hbECM with the goal of improving the mechanical stability (Fig. 2a, Table 1). The combination of the two materials was found to induce rapid gelation which prevented homogeneous mixing. Following Wang and co-workers [21], the inclusion of ASAP improved the dispersion efficiency of LAP, thus we assessed whether ASAP would cause similar improvements upon mixing with the novel hbECM. The selective inclusion of ASAP significantly increased the transparency of the nanocomposite gel (Fig. 2b), as demonstrated by the micrographs and the reduction in absorbance to a level comparable with the hbECM transparent gel. However, while this created clearer gels, the inclusion of ASAP hindered rather than enhanced nanoclay interactions with proteins within the hbECM.

Thus, the overall effect of ASAP was to reduce the storage moduli of the gels. Indeed, a similar trend was found for the storage moduli of the nanocomposites with varying ASAP concentration (Fig. 2c),

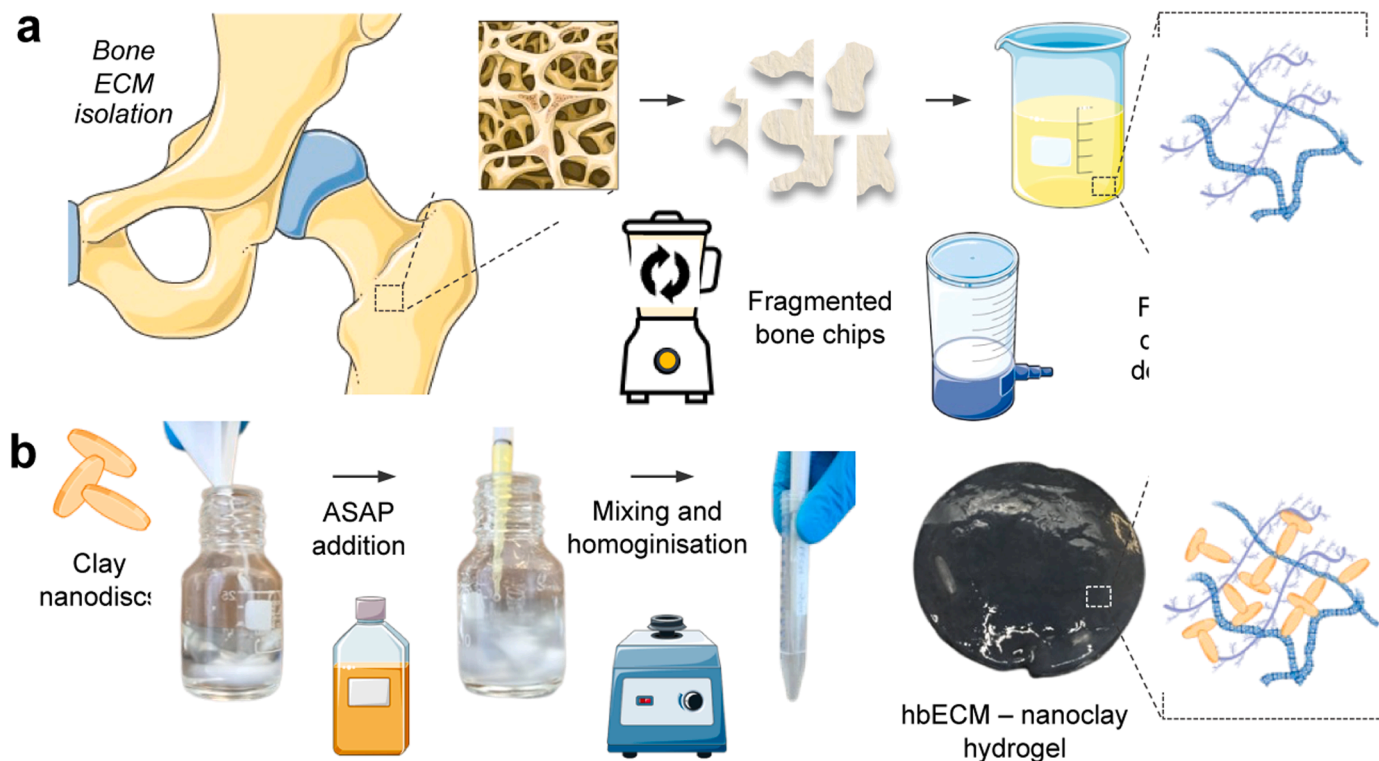


Fig. 1. Preparation process of hbECM, nanoclay (Laponite) and composite hydrogels. a) Human bone ECM gel was created from trabecular bone collected from femoral heads, grounded, and demineralized under agitation with organic solvents and filtered. Decellularization was carried out in a step-wise manner to completely remove cellular material. Nanoclay gels (b) were engineered by suspending Laponite® powder in ultrapure water and sheared while adding ASAP solution. Nanocomposite gels were prepared by mixing the Nanoclay suspensions with ECM digest supernatant prior neutralization.

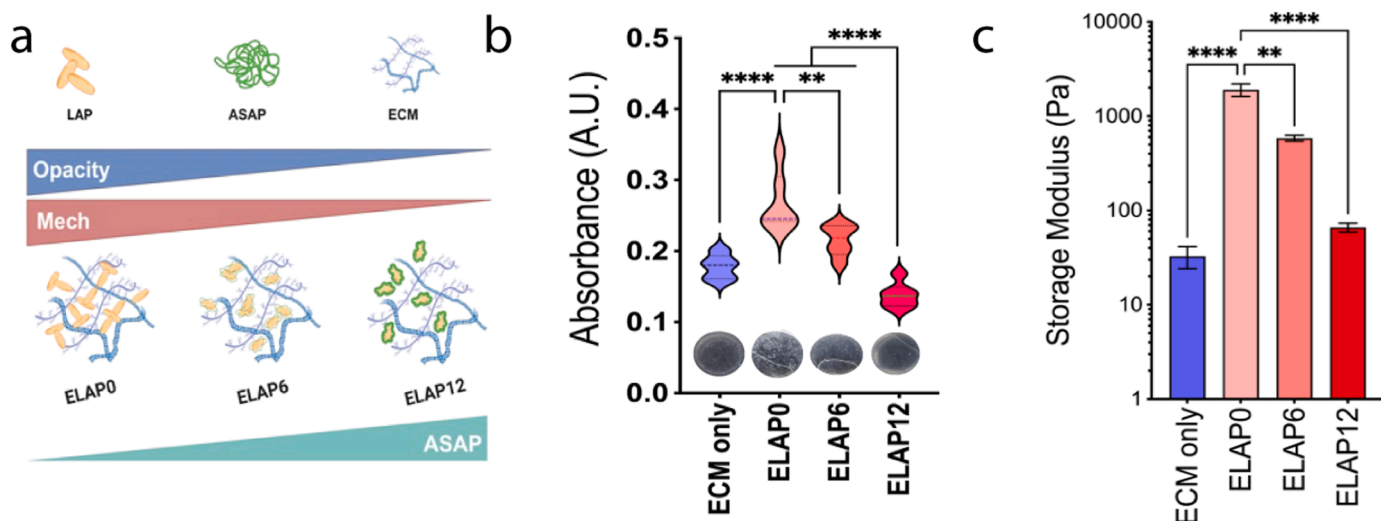


Fig. 2. The effects of combining Laponite and the human bone extracellular matrix hydrogel on the physical properties of the gels (a). A turbidimetric assay (b) of ECM gels and composites absorbance to light exposure, demonstrating transparency. Storage moduli (c) of ECM only and composite gels measured in the linear viscoelastic region of the gels during an amplitude sweep.

demonstrating the ability of ASAP to control the ultimate clay-protein assembly. With a reduced layer-to-layer interaction between the clay particles, the composites were mechanically weaker, resulting in gels with reduced mechanical competency. The ECM gel alone was observed to be poorly stable, however, the inclusion of nanoclay augmented the stability and storage modulus of the gel. Indeed, as previously reported [22], the long-chained ASAP can coat the positively charged outer rim of LAP, and with a dose-dependent effect prevent the stacking of the nanoparticles while improving dispersion (Fig. 3a). To investigate the effects of exogenous addition of blood serum on rheological properties of the nanocomposite gel, FBS was placed in contact with a varying concentration of hbECM-clay gels with an increasing amount of ASAP. In accordance with published articles [23], results (Fig. 3b) demonstrated a significant increase of storage modulus following exposure to FBS. This responsive gelation to physiological fluids seen with ASAP, suggests interesting potential for use as a minimally invasive injectable scaffold

for bone regeneration.

The composites including ASAP demonstrated low initial viscosity, allowing injection using a needle. Moreover, when exposed to physiological fluids in the body, the nanocomposite gel was observed to stiffen and set into a solid state (Fig. 3b), that retained its shape and displayed mechanical stability. Limited inclusion of ASAP (ELAP0 and ELAP6) supported a non-significant change in storage modulus.

In contrast, the inclusion of a greater concentration of ASAP (ELAP12) showed a substantial increase in storage modulus after the addition of FBS, while demonstrating a lower overall modulus at regime, suggesting a dose dependent reaction. The inclusion of protein-rich ECM combined with the attraction-repulsion nature of the composite (Fig. 3c) demonstrates the tuning ability of the nanocomposite to adapt to protein retention depending on the presence of ASAP. This property offers a novel injectable gel, applicable in a minimally-invasive approach, with the potential to reduce surgery time and size of incisions as well as the

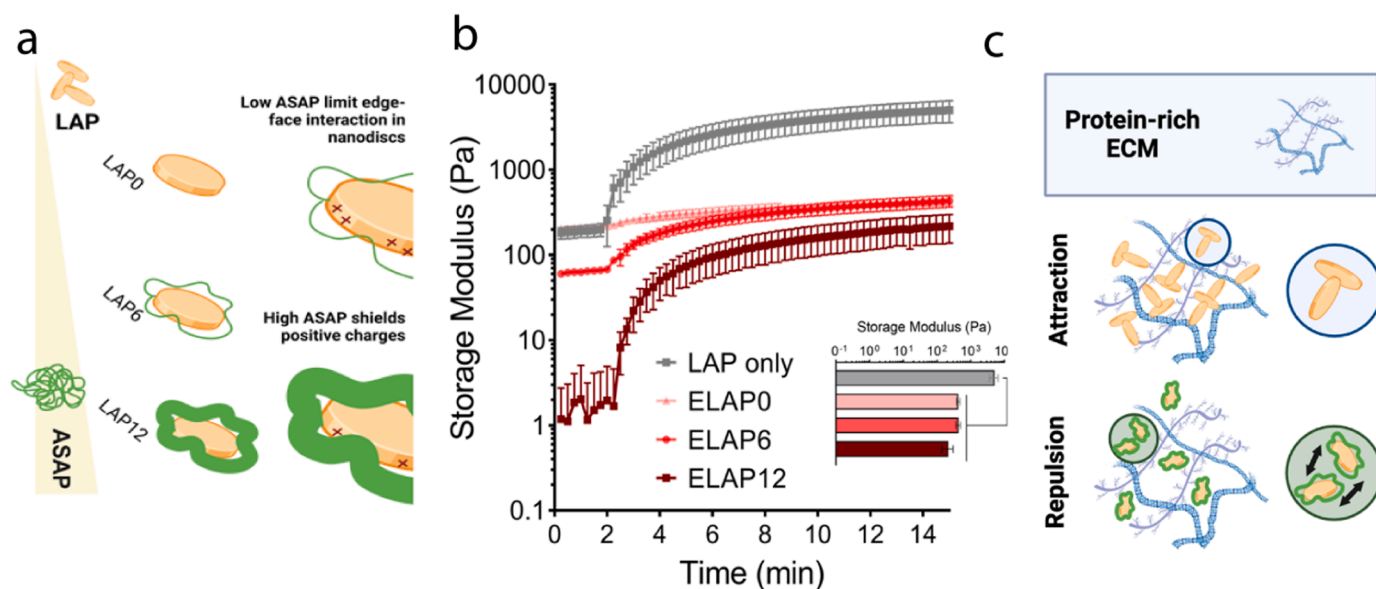


Fig. 3. Investigation of the rheological modification of blood serum to nanocomposite (a) gels. Constant strain of composite gels (b) with FBS added after 2 minutes, displayed a stiffening effect of the gels in response to physiological fluids. Overall mechanisms of LAP-ASAP-hbECM interaction illustrated in (c). Statistical significance assessed by one-way ANOVA. Mean \pm S.D. $n=3$, ** $p<0.01$, **** $p<0.001$, **** $p<0.0001$.

potential to reduce infection rates as observed with current bone graft techniques [24].

To assess ECM stability in physiological solution (Fig. 4a), injectable nanocomposite and control gels were incubated for 24 h. Following an exposure to collagenase, a burst release of protein was observed for ECM only, indicating a rapid enzymatic degradation of ECM hydrogel (Fig. 4b). In contrast, ECM hydrogel containing Laponite® (ELAP0) displayed a slow release of proteins. The nanoclay was capable of crosslinking the proteins in hbECM gel, minimising the cleavage of ECM proteins by the collagenase enzymes, facilitating the maintenance of a stable structure following gelation. Thus, the composite gels were found to retain greater structural integrity with reduced degradation in physiological conditions (Fig. 4b). During the incubation in PBS and collagenase, no difference in pH was observed, as well as no significant weight loss of composite gels (Supplementary Fig. 3). However, a significant release of ECM proteins was detected from the composite gels during the incubation, particularly following collagenase treatment (Fig. 4b) suggesting that the released amount of ECM from the composite gels was insignificant to affect the weight change and pH in the solution.

The ability to control the gel degradation process, enabled tuning and modulation of the rate at which the endogenous growth factors could be released from the ECM. The increased molecular interactions between the clay nanoparticles and the hbECM proteins resulted in stiffer gels, while contributing to reduced degradation rate of composite gels. Critically, the modulation of the interaction of nanoclay with hbECM, ensured the exposure of bone proteins could be regulated limiting enzyme degradation and thus tuning gel degradation and, ultimately, protein release.

3.3. Composite gels support promyoblast C2C12 cell spreading and facilitate osteogenic differentiation with ALP release

Classic studies of demineralised bone matrix highlight the potential of hbECM derived gels as a repository of bone inductive molecules and instructive extracellular matrix motifs [10] with the potential to induce osteoinduction. Hydrogel materials are versatile and capable of influencing cellular morphology *in vitro*. As a direct effect of composite rheological

To assess this potential *in vitro*, C2C12 myoblasts were seeded on hbECM gels with and without addition of LAP and/or ASAP (Fig. 5a, i-ii). Cell spreading was first assessed in LAP-hbECM composites

containing various concentrations of ASAP. Interestingly, a modest improvement in cell spreading was apparent with addition of ASAP. This could be related to the increase in charge depletion by ASAP shielding the nanoclay rim, limiting the close interaction between nano-platelets, thus reducing the mechanical properties. C2C12 cells seeded on gels with increasing concentration of ASAP were found to express ALP following 3 days of culture in comparison to control and nanocomposite gels (Fig. 5b).

An increasing concentration of BMP-2 was found to drive enhanced ALP expression in all treatment groups. In the absence of BMP-2, ALP expression was negligible, while in the presence of increasing BMP-2 concentrations, the synergistic combination of hbECM and LAP was found to elicit a greater response compared to hbECM controls ($p < 0.0001$), independently of the ASAP concentration (Fig. 5c). These results indicate the composite gels facilitate pro-myoblast C2C12 osteogenic differentiation with a dose-dependent effect due to BMP-2 concentration. The hbECM-based nanocomposite offers new possibilities for the encapsulation and retention of BMP-2, resulting in an ASAP-mediated modulation of binding affinity and steric inclusion due to the attraction-repulsion mechanism previously reported (Fig. 5d).

4. Conclusion

We demonstrated that human bone ECM offers significant potential in bone regeneration applications and the addition of nanoclay confers useful advantages in hECM handling and physicochemical properties. However, while the further addition of ASAP improved nanoclay dispersion within hbECM and facilitated serum responsive gelation, it interfered with the interaction of nanoclay with hECM as well as BMP-2. This suggests that the hbECM-LAP composite without ASAP is an effective design for delivering BMP-2 molecules and enhancing osteoinductive properties. Future work will focus on investigating the closer interactions between the components using XRD analysis, while studying possible intracellular effects via TEM investigation, and lastly optimizing the hbECM-LAP composite to enhance its effects and determine its therapeutic efficacy in bone repair.

Author statement

We can confirm that this manuscript has neither been published nor is currently under consideration for publication either in whole or in

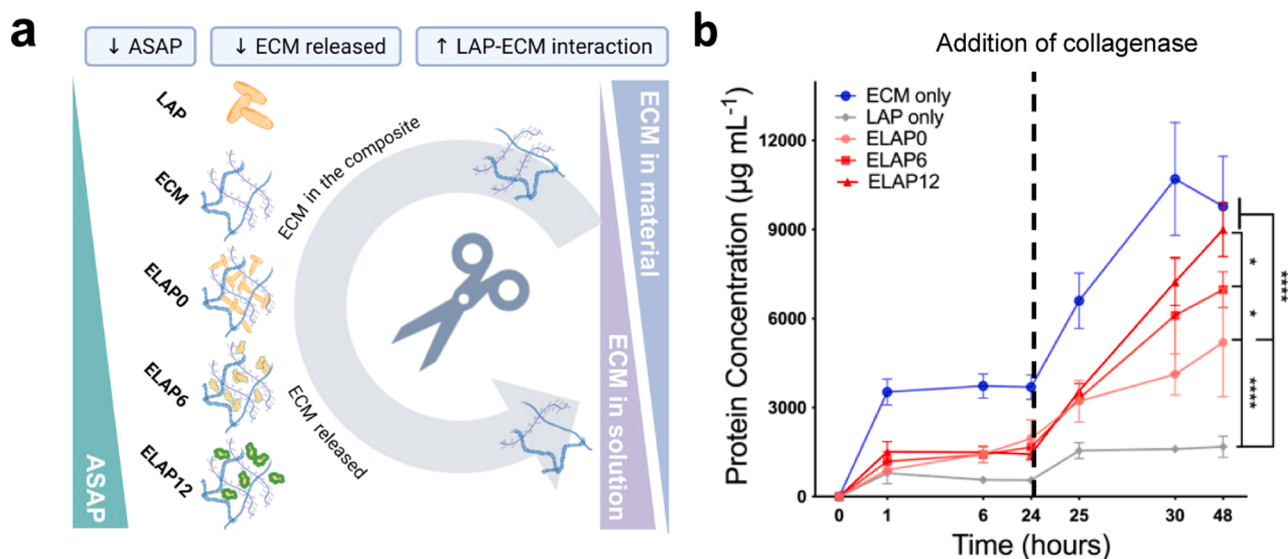


Fig. 4. Study of the enzymatic degradation of nanocomposite gels (a). The percentage of released proteins from the nanocomposite gels (b) over 48 h cultivating gels in PBS for 24 h then exposing the groups to collagenase to 24 h to imitate *in vivo* conditions. Statistical significance assessed by one-way ANOVA. Mean \pm S.D. $n=3$, * $p < 0.05$, **** $p < 0.0001$.

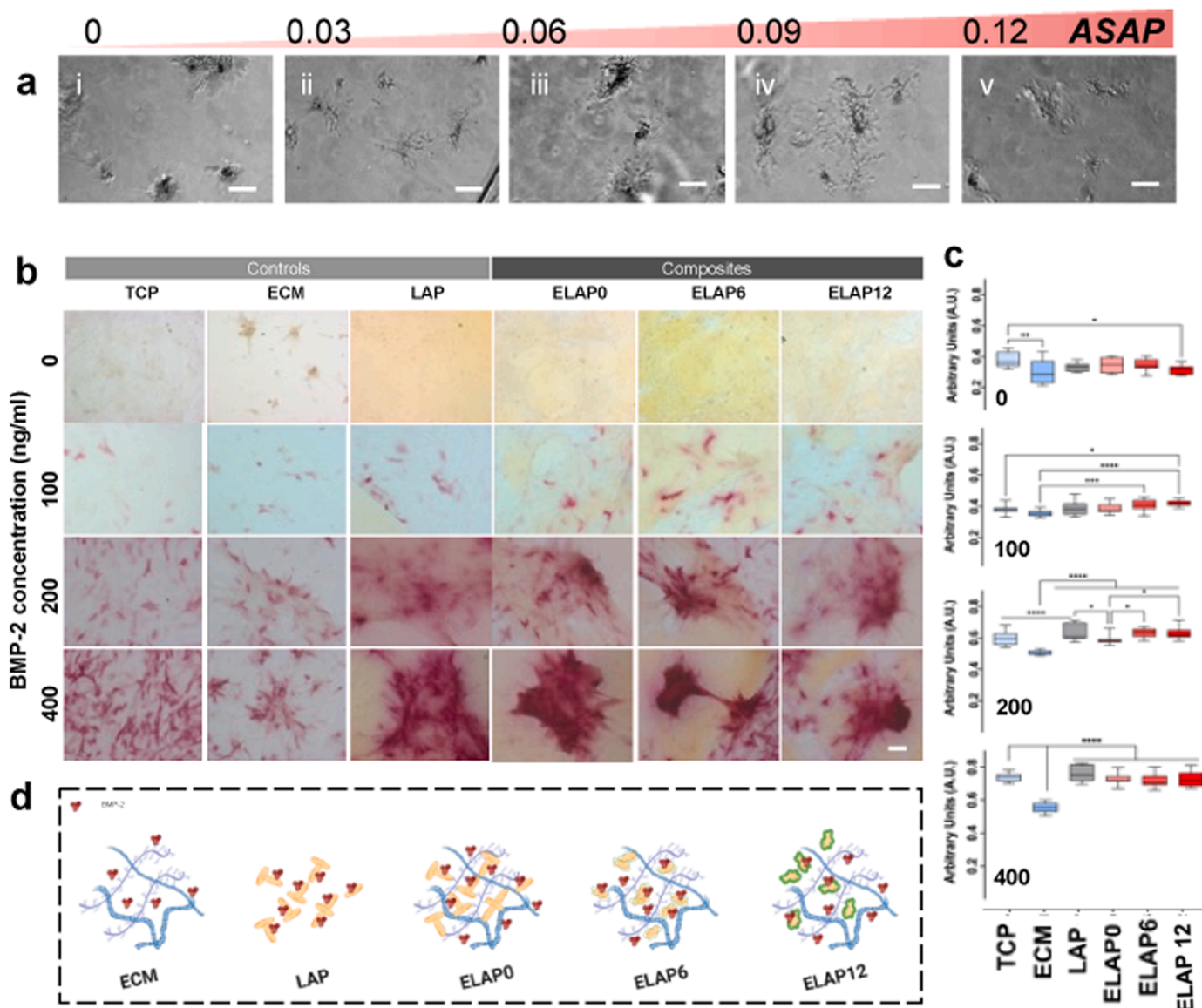


Fig. 5. Functionality of nanocomposite gels in the presence of cells. Morphological appearance of seeded cells on nanocomposite gels. (a,i-v) Brightfield images of C2C12 seeded on growing concentration of ASAP dispersed in clay-hbECM composites. Cell spreading is consistent with ASAP concentration, with no apparent difference in elongation and spreading. (b) ALP staining of C2C12 seeded on controls (tissue culture plastic, ECM and Laponite®) and composite gels with growing concentration of BMP-2 (0, 100, 200, 400 ng ml⁻¹). Measurements (b) of ALP intensity. Schematic representation (d) of the possible synergistic interaction of BMP-2 loaded in nanocomposite ECM-based materials. Scale bars: 50 μ m, 100 μ m. Statistical significance assessed by one-way ANOVA. Mean \pm S.D. n=3, * p<0.05, ***p<0.001, **** p<0.0001.

part, by any other journal. The submission has been approved by each coauthor.

Notes

R Oreffo and J.I. Dawson are co-founders and shareholders in a university spin out company with a license to IP indirectly related to the current manuscript.

CRediT authorship contribution statement

Yang-Hee Kim: Writing – review & editing, Writing – original draft, Visualization, Validation, Supervision, Resources, Project administration, Methodology, Investigation, Formal analysis, Data curation, Conceptualization. **Jonathan I Dawson:** Writing – review & editing, Writing – original draft, Supervision, Resources, Project administration,

Methodology, Funding acquisition, Data curation, Conceptualization. **Richard O C Oreffo:** Writing – review & editing, Writing – original draft, Supervision, Resources, Project administration, Funding acquisition, Conceptualization. **Janos M. Kanczler:** Writing – review & editing, Writing – original draft, Validation, Methodology, Investigation, Data curation. **Alessandro Nucara:** Data curation, Investigation. **Valeria Giliberti:** Data curation, Formal analysis, Investigation, Methodology. **Julietta V Rau:** Data curation, Formal analysis, Methodology. **Lucia Iafrate:** Data curation, Formal analysis, Methodology. **Vikash H Dodhia:** Writing – original draft, Methodology, Investigation. **Gianluca Cidonio:** Writing – review & editing, Writing – original draft, Visualization, Validation, Supervision, Methodology, Investigation, Formal analysis, Data curation, Conceptualization.

Declaration of Competing Interest

The authors declare the following financial interests/personal relationships which may be considered as potential competing interests: Jonathan Dawson reports financial support was provided by Engineering and Physical Sciences Research Council. Jonathan Dawson and Richard Oreffo reports a relationship with Renovos Biologics Limited that includes: board membership and equity or stocks. If there are other authors, they declare that they have no known competing financial interests or personal relationships that could have appeared to influence the work reported in this paper.

Data availability

Data will be made available on request.

Acknowledgements

This study was supported by grants from MTF Biologics (OSTEO-MIMIC) awarded to GC, the Biotechnology and Biological Sciences Research Council (BBSRC LO21071/ and BB/L00609X/1) and UK Regenerative Medicine Platform Hub Acellular Approaches for Therapeutic Delivery (MR/K026682/1) Acellular Hub, SMART Materials 3D Architecture (MR/R015651/1) and the UK Regenerative Medicine Platform (MR/L012626/1 Southampton Imaging) to RO and MRC-AMED Regenerative Medicine and Stem Cell Research Initiative (MR/V00543X/1) to JID, RO and YK.

Appendix A. Supporting information

Supplementary data associated with this article can be found in the online version at [doi:10.1016/j.mtcomm.2024.109082](https://doi.org/10.1016/j.mtcomm.2024.109082).

References

- [1] A. Cieza, K. Causey, K. Kamenov, S.W. Hanson, S. Chatterji, T. Vos, Global estimates of the need for rehabilitation based on the Global Burden of Disease study 2019: a systematic analysis for the Global Burden of Disease Study 2019, *Lancet* 396 (10267) (2020) 2006–2017, [https://doi.org/10.1016/S0140-6736\(20\)32340-0](https://doi.org/10.1016/S0140-6736(20)32340-0).
- [2] B. Dozza, F. Salamanna, M. Baleani, et al., Nonunion fracture healing: evaluation of effectiveness of demineralized bone matrix and mesenchymal stem cells in a novel sheep bone nonunion model, *J. Tissue Eng. Regen. Med* 12 (9) (2018) 1972–1985, <https://doi.org/10.1002/term.2732>.
- [3] L. Iafrate, M.C. Benedetti, S. Donsante, et al., Modelling skeletal pain harnessing tissue engineering, *Vitr. Models* 1 (4-5) (2022) 289–307, <https://doi.org/10.1007/s44164-022-00028-7>.
- [4] H.S. Sohn, J.K. Oh, Review of bone graft and bone substitutes with an emphasis on fracture surgeries, *Biomater. Res* 23 (1) (2019) 4–10, <https://doi.org/10.1186/s40824-019-0157-y>.
- [5] D. van der Heide, G. Cidonio, M.J. Stoddart, M. D'Este, 3D printing of inorganic-biopolymer composites for bone regeneration, *Biofabrication* 14 (4) (2022) 042003, <https://doi.org/10.1088/1758-5090/ac8cb2>.
- [6] L. Iafrate, M.C. Benedetti, S. Donsante, et al., Modelling skeletal pain harnessing tissue engineering, *Vitr. Models* 1 (4-5) (2022) 289–307, <https://doi.org/10.1007/s44164-022-00028-7>.
- [7] F. Bini, A. Pica, A. Marinozzi, F. Marinozzi, A 3D model of the effect of tortuosity and constrictivity on the diffusion in mineralized collagen fibril, *Sci. Rep.* 9 (1) (2019), <https://doi.org/10.1038/s41598-019-39297-w>.
- [8] A. Smandri, M.E. Al-Masawa, N.M. Hwei, M.B. Fauzi, ECM-derived biomaterials for regulating tissue multicellularity and maturation, *iScience* 27 (3) (2024) 109141, <https://doi.org/10.1016/j.jsci.2024.109141>.
- [9] M.T. Spang, K.L. Christman, Extracellular matrix hydrogel therapies: in vivo applications and development, *Acta Biomater.* 68 (2018) 1–14, <https://doi.org/10.1016/j.actbio.2017.12.019>.
- [10] M.R. Urist, Bone: formation by autoinduction, *Science* (1979) 150 (3698) (1965) 893–899, <https://doi.org/10.1126/SCIENCE.150.3698.893>.
- [11] S.F. Badyal, The extracellular matrix as a biologic scaffold material, *Biomaterials* 28 (25) (2007) 3587–3593, <https://doi.org/10.1016/j.biomaterials.2007.04.043>.
- [12] Y. Zhao, H. Peng, L. Sun, et al., The application of small intestinal submucosa in tissue regeneration, *Mater. Today Bio* 26 (2024) 101032, <https://doi.org/10.1016/j.mtbio.2024.101032>.
- [13] Y.H. Kim, J.M. Kanczler, S. Lanham, et al., Biofabrication of nanocomposite-based scaffolds containing human bone extracellular matrix for the differentiation of skeletal stem and progenitor cells, *Biores Manuf.* 7 (2) (2024) 121–136, <https://doi.org/10.1007/s42242-023-00265-z>.
- [14] G. Cidonio, M. Glinka, Y.H. Kim, J.I. Dawson, R.O.C. Oreffo, Nanocomposite clay-based bioinks for skeletal tissue engineering, in: A. Rainer, L. Moroni (Eds.), *Computer-Aided Tissue Engineering: Methods and Protocols*, Springer US, 2021, pp. 63–72, https://doi.org/10.1007/978-1-0716-0611-7_6.
- [15] J. Labanda, J. Sabaté, J. Llorens, Rheology changes of Laponite aqueous dispersions due to the addition of sodium polyacrylates of different molecular weights, *Colloids Surf. A Physicochem. Eng. Asp.* 301 (1-3) (2007) 8–15, <https://doi.org/10.1016/j.colsurfa.2007.01.011>.
- [16] T.B. Becher, M.C.P. Mendonça, M.A. de Farias, R.V. Portugal, M.B. de Jesus, C. Ornelas, Soft nanohydrogels based on laponite nanodiscs: a versatile drug delivery platform for theranostics and drug cocktails, *ACS Appl. Mater. Interfaces* 10 (26) (2018) 21891–21900, <https://doi.org/10.1021/acsami.8b06149>.
- [17] D. Choi, J. Heo, J. Aviles Milan, et al., Structured nanofilms comprising Laponite® and bone extracellular matrix for osteogenic differentiation of skeletal progenitor cells, *Mater. Sci. Eng. C* 118 (August 2020) (2021) 111440, <https://doi.org/10.1016/j.msec.2020.111440>.
- [18] Kim Y.H., Kanczler J.M., Lanham S., et al. Biofabrication of nanocomposite-based scaffolds containing human bone extracellular matrix for the differentiation of skeletal stem and progenitor cells. *bioRxiv*. Published online January 1, 2023: 2023.04.07.536074. doi:10.1101/2023.04.07.536074.
- [19] G. Cidonio, M. Cooke, M. Glinka, J.I. Dawson, L. Grover, R.O.C. Oreffo, Printing bone in a gel: using nanocomposite bioink to print functionalised bone scaffolds, *Mater. Today Bio* 4 (2019) 100028, <https://doi.org/10.1016/j.mtbio.2019.100028>.
- [20] Kim Y.H., Cidonio G., Kanczler J.M., Oreffo R.O.C., Dawson J.I. Human bone tissue-derived ECM hydrogels: controlling physicochemical, biochemical, and biological properties through processing parameters, *bioRxiv*. Published online January 1, 2023:2023.08.03.551765. doi:10.1101/2023.08.03.551765.
- [21] Q. Wang, J.L. Mynar, M. Yoshida, et al., High-water-content mouldable hydrogels by mixing clay and a dendritic molecular binder, *Nature* 463 (7279) (2010) 339–343, <https://doi.org/10.1038/nature08693>.
- [22] Q. Wang, J.L. Mynar, M. Yoshida, et al., High-water-content mouldable hydrogels by mixing clay and a dendritic molecular binder, *Nature* 463 (7279) (2010) 339–343, <https://doi.org/10.1038/nature08693>.
- [23] P. Shi, Y.H. Kim, M. Mousa, R.R. Sanchez, R.O.C. Oreffo, J.I. Dawson, Self-assembling nanoclay diffusion gels for bioactive osteogenic microenvironments, *Adv. Health Mater.* 7 (15) (2018) 1800331, <https://doi.org/10.1002/adhm.201800331>.
- [24] G.M. Calori, E. Mazza, M. Colombo, C. Ripamonti, L. Tagliabue, Treatment of long bone non-unions with polytherapy: indications and clinical results, *Injury* 42 (6) (2011) 587–590, <https://doi.org/10.1016/j.injury.2011.03.046>.